JACS
JOURNAL OF THE AMERICAN CHEMICAL SOCIETY
pubs.acs.org/JACS
Article

An Analysis of the Binding Function and Structural Organization of the Protein Corona

Yuwei Zhang, Jamie L. Y. Wu, James Lazarovits, and Warren C. W. Chan*

Cite This: J. Am. Chem. Soc. 2020, 142, 8827−8836

ABSTRACT: Blood proteins adsorb onto the surface of nanoparticles after intravenous injection to form a protein corona. The underlying organization and binding function of these adsorbed proteins remain unclear. This can impact how the corona mediates cell and tissue interactions. Here, we investigated the function and structural organization of the protein corona using an immunoassay approach. We discovered that only 27% of the adsorbed proteins examined are functional for binding to their target protein. This is because the corona architecture is not a monolayer, but an assembly of proteins that are bound to each other. We further demonstrated that we can control the binding functionality of a protein by changing the organization of proteins in the assembly. We show that manipulation of the corona protein composition and assembly can influence their interactions with macrophage cells in culture. This study provides detailed functional and structural insights into the protein corona on nanomaterials and offers a new strategy to manipulate it for controlled interactions with the biological system.

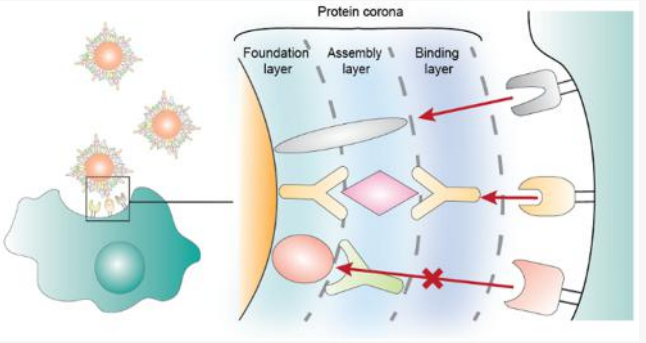

INTRODUCTION

Nanoparticles are engineered to deliver therapeutic agents to diseased tissues.[1−3] The material, size, shape, and surface chemistry of nanoparticles for specific medical applications are heavily investigated.[4] These physicochemical properties can affect the nanoparticle's pharmacokinetics, biodistribution,[5] toxicity,[6] and cellular interactions.[7] After administering nanoparticles into the bloodstream, they are immediately in contact with the surrounding serum proteins.[8,9] These proteins rapidly adsorb onto nanoparticles and form a layer, termed the protein corona.[10−12] It has been shown that these adsorbed proteins can replace nanoparticles' engineered surfaces[13] and alter their biological interactions.[14−16]

There have been tremendous efforts in profiling the adsorbed serum proteins. Cullis and co-workers used poly(acrylamide) gel electrophoresis (PAGE) and immunoblotting to analyze the protein corona on liposomes and found that few of the adsorbed proteins correlated with a liposome's half-life in vivo.[17] Tenzer and Walkey and co-workers applied label-free shotgun tandem mass spectrometry (LC-MS/MS) to systematically profile and quantify the protein corona.[18,19] Over 300 different species of serum proteins were found on the surface of silica and gold nanoparticles. In the past five years, researchers have started to use this approach to identify serum proteins adsorbed to nanoparticles with different materials, sizes, shapes, and surface chemistries.[20−22]

Despite a significant number of studies on the corona in the last 30 years, only a few examined the structure and binding function of the serum adsorbed proteins. Dawson et al. used metal nanoparticle-labeled antibodies and transmission electron microscopy (TEM) to visualize the adsorbed proteins on polystyrene nanoparticles.[23] Similarly, Landry et al. used stochastic optical reconstruction microscopy to look at the distribution of proteins on silica nanoparticles.[24] These studies provided the spatial mapping of proteins on the nanoparticle surface, but the structural organization of specific proteins on the nanoparticle surface is unknown. Moreover, whether the proteins can bind to their target receptor is still unclear. Here, we provide a more detailed analysis of the function and structure of the protein corona by quantifying the binding function of adsorbed proteins and determine their structural organization.

Our research workflow involves first profiling the protein composition of the protein corona using LC-MS/MS. We adopted the enzyme-linked immunosorbent assay (ELISA) to quantify the proteins that are functional for binding. We also used chemical etchant to release the adsorbed proteins and determined their structural organization. Once we identified

Received: February 16, 2020
Published: April 15, 2020

https://dx.doi.org/10.1021/jacs.0c01853
J. Am. Chem. Soc. 2020, 142, 8827−8836

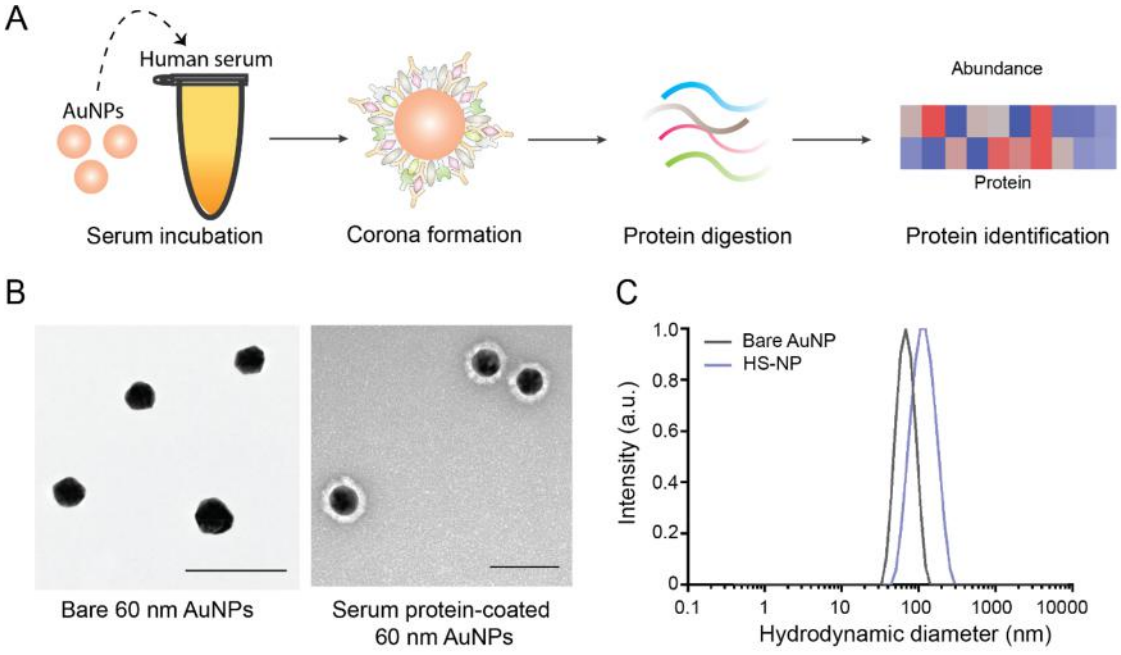

D

Uniprot ID	Protein name	Abbr.	Rel. Abun.	Uniprot ID	Protein name	Abbr.	Rel. Abun.
P01024	Complement C3	C3	5.10%	P18428	Lipopolysaccharide-binding	LBP	0.72%
P01008	Antithrombin-III	ATIII	3.97%	P01009	Alpha-1-antitrypsin	SER	0.64%
P02751-8	Fibronectin	FN	3.72%	P02788	Lactotransferrin	TF	0.62%
P08603	Complement factor H	CFH	2.52%	P27918	Properdin	CFP	0.57%
P02671 (+1)	Fibrinogen	FIB	1.75%	P02775	Platelet basic protein	PBP	0.52%
P03952	Plasma kallikrein	PK	1.74%	P03950	Angiogenin	ANG	0.46%
P12259	Coagulation factor V	FV	1.49%	P02652	Apolipoprotein A-II	APOA2	0.44%
P02776	Platelet factor 4	PF4	1.31%	P00488	Coagulation factor XIII	FXIII	0.39%
P0C0L5	Complement C4-B	C4	1.23%	P02656	Apolipoprotein C-III	APOC3	0.33%
P10909-2	Clusterin	CLU	1.21%	O00602	Ficolin-1	FCN	0.26%
P03951	Coagulation factor XI	FXI	1.15%	P68871	Hemoglobin	HEM	0.23%
P01857	Immunoglobulin G	IgG	0.97%	P02766	Transthyretin	PALB	0.20%

Figure 1. Characterization and profiling of adsorbed serum proteins on gold nanoparticles. (A) 60 nm gold nanoparticles were incubated with the human serum to form the protein corona. Serum protein-coated nanoparticles were isolated with the unbound proteins. Adsorbed proteins were denatured and reduced to peptides. The peptides were characterized by label-free liquid chromatography-tandem mass spectrometry (LC-MS/MS). (B) Transmission electron microscopy images of nanoparticles before (left) and after (right) the serum protein coating. The protein adsorption layer was negatively stained with uranyl acetate. Scale bar: 100 nm. (C) The hydrodynamic diameter of the nanoparticles before and after the human serum (HS) protein coating determined by dynamic light scattering (DLS). (D) The list of 24 proteins that were selected for the quantification of their binding functionality. The selection was based on their abundance in the corona and the commercial availability of their antibodies, antibody-coated wells, and standards. The abbreviations for proteins (abbr.) used in this study and their relative abundance (Rel. Abun) are listed.

the protein structure of the corona, we demonstrate the manipulation of the structure of protein corona to mediate cellular interaction.

RESULTS AND DISCUSSION

We first prepared serum protein-coated spherical gold nanoparticles (AuNPs) and profiled the composition of adsorbed proteins as shown in Figure 1A. This allows us to determine a list of proteins as candidates to quantify their binding functionality. Experimentally, 60 nm spherical gold nanoparticles (AuNPs) were synthesized using a citrate reduction method and incubated with human serum. After the incubation, we isolated protein-coated nanoparticles from the unbound protein by centrifugation and washed them with Tween-20 supplemented PBS (PBST). The protein coating on nanoparticles was observed with transmission electron microscopy (TEM) (Figure 1B). Using UV−vis, we also showed that protein-coated nanoparticles are colloidal stable in 1× PBS (Figure S1). We quantified the increase of AuNPs' hydrodynamic diameter (HD) with dynamic light scattering (DLS) (Figure 1C). We found that the serum protein corona added 30 ± 13 nm to the nanoparticle diameter. The protein composition of this layer was profiled using label-free LC-MS/MS. A total of 288 different human serum proteins were identified as shown in the heat map (Figure S2). We sorted the proteins according to their abundance and found that the top 80 most abundant proteins represent 93% of the whole corona. We chose these proteins as candidates for quantifying their binding functionality.

We used an enzyme-linked immunosorbent assay (ELISA)[25] to measure the binding function of the adsorbed proteins. It requires commercially available primary and secondary anti-

https://dx.doi.org/10.1021/jacs.0c01853
J. Am. Chem. Soc. 2020, 142, 8827−8836

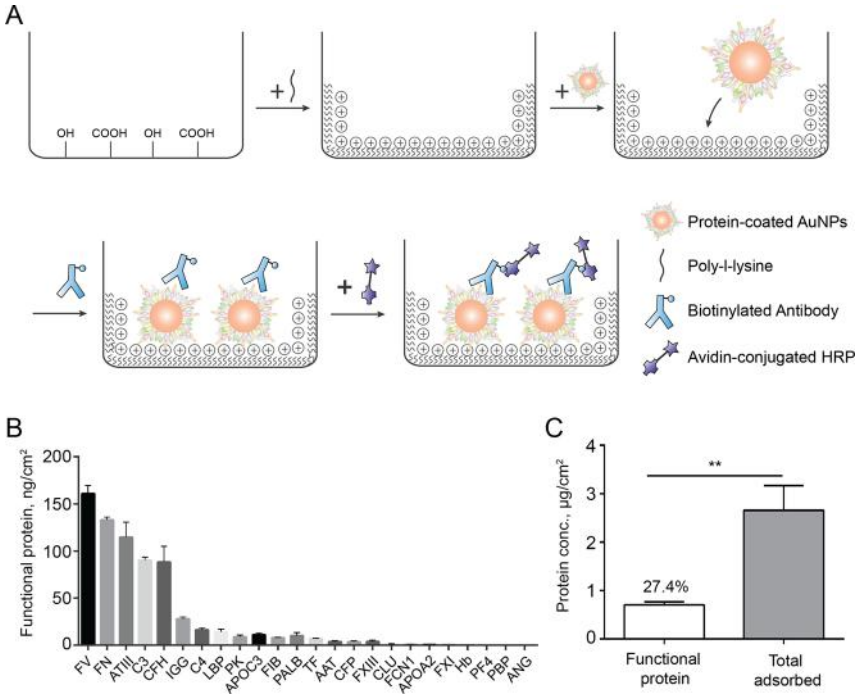

Figure 2. Quantification of the binding functionality of proteins in nanoparticle protein corona. (A) Schematics of the enzyme-linked immunosorbent assay (ELISA) for protein functionality quantification. The plasma-treated wells were first coated with poly L-lysine to render the surface positively charged. Serum protein-coated nanoparticles were incubated and allowed adsorption to the well. The biotinylated antibody was added to bind with the target protein. This was followed by the addition of avidin-conjugated horseradish peroxidase (HRP). A standard curve was prepared for the target protein in separate wells under the traditional sandwich assay format. (B) The concentration of the 24 proteins that are functional for binding in the protein corona. The result was normalized to the surface area of nanoparticles adsorbed on the well, determined by inductively coupled plasma mass spectrometry (ICP-MS). (C) The total amount of the binding functional proteins compared to their total adsorbed amount. The total adsorbed amount for the 24 proteins was determined through their relative abundance

bodies, antibody-coated wells, and free protein standards. We tried to obtain these components for all 80 proteins and found that only 24 of them have the required assay components to compare the binding. The 24 proteins are listed in Figure 1D. Though this is not ideal, this allowed us to determine the binding function across these proteins consistently using the same method. These 24 proteins tested for their binding function represent 33% of the whole corona (Figure S3). We hope that similar assay designs can be done for the other corona proteins to allow a more thorough analysis.

Figure 2A shows the workflow schematic for quantifying the nanoparticle corona proteins that are functional for binding to target ligands. The serum protein-coated 60 nm gold nanoparticles were first immobilized onto a 96-well plate. These well plates were precoated with positively charged poly L-lysine (PLL). Since the serum protein-coated nanoparticles were negatively charged (Figure S4), they can be electrostatically immobilized onto the well (Figure S5a). The coating is also consistent with an average 5% coefficient of variation (CV) for immobilizing nanoparticles (Figure S5b). Any unbound nanoparticles were washed away with Tween-20 supplemented PBS (PBST). We next added biotinylated antibodies that specifically target one of the 24 proteins. The antibody binds specifically to proteins on the nanoparticles that can bind to their target protein. Avidin-conjugated horseradish peroxidase (HRP) was added to bind to the biotinylated antibodies. This allows the HRP to be attached to the protein complex of the target protein and biotinylated antibody. The substrate for HRP, tetramethylbenzidine (TMB), was then added to the well. The HRP oxidizes the substrate and generates a colorimetric signal with a peak absorbance at 450 nm that can be measured using an absorbance plate reader.[26] We converted the colorimetric signal to the concentration of binding functional proteins from a standard curve. The standards consist of known concentrations of free proteins. These proteins were captured onto the wells that were precoated with their antibody. Biotinylated antibody and Avidin-conjugated HRP were added to bind with the captured free protein standards. Both HRP on nanoparticles and free protein standards were allowed to react with TMB for the same amount of time. This allows us to quantify the amount of binding functional proteins by comparing the signal from nanoparticles to the standards.

We first validated this quantification method with Immunoglobulin-coated nanoparticles (IgG-NPs) (Figure S6). IgG-NPs can be prepared with a range of surface coverage as shown in Figure S7. We then applied our assay to these IgG-NPs to quantify the number of IgG. Because this is a single protein system, all proteins are expected to be functional for binding. Figure S8 shows that our assay can quantify the IgG on nanoparticle regardless of the protein coverage. If the IgG is sterically covered by anti-IgG, the assay shows no signal (Figure S9). If the IgG is partially denatured, the assay also shows decreased signal (Figure S10). This confirms that we only quantified proteins that are functional for binding. This allows us to move onto applying the assay to the selected 24 proteins in the protein corona of nanoparticles.

Figure 2B shows the quantification of the number of corona proteins that are functional for binding. The concentration was normalized to the surface area of nanoparticles to compare

https://dx.doi.org/10.1021/jacs.0c01853
J. Am. Chem. Soc. 2020, 142, 8827−8836

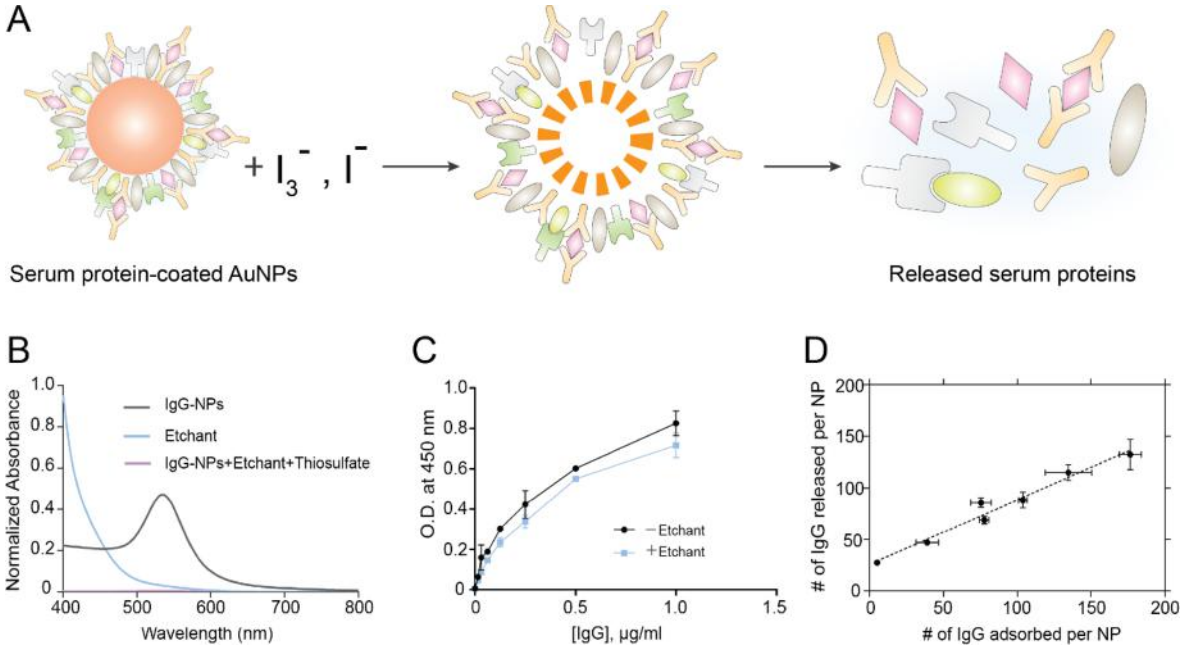

Figure 3. Optimization and validation of nondenaturing release of adsorbed serum proteins for structural analysis of the protein corona. (A) Schematics of the assay for releasing adsorbed proteins through chemically etching away the gold core of nanoparticles. Serum protein-coated nanoparticles were incubated with the iodine and iodide ion solution. After the gold core was etched away, the released serum proteins were obtained. (B) The UV−vis absorbance spectrum of the Immunoglobulin G-coated 60 nm gold nanoparticles (IgG-NPs) before and after the addition of the etchant. Thiosulfate was added to remove the residue iodine. (C) The effect of etchant on the native structure and function of proteins. Human IgG in PBS before (− etchant) and after (+ etchant) incubating the etchant solution was tested with the traditional sandwich ELISA. The O.D. represents the absorbance of the TMB substrate at 450 nm. No significant difference was observed after the addition of the etchant. The standard deviation of two technical replicates was also shown. (D) A correlation plot between the number of IgG released through the etching and the number of IgG total adsorbed on NPs (n = 3; Pearson correlation coefficient: 0.9841). The number of IgG adsorbed per NP was quantified by Bicinchoninic acid assay after denaturing and extracting adsorbed proteins. The number of IgG released per NP was quantified with traditional sandwich ELISA after the gold nanoparticle core was etched.

their binding functionality. This is achieved through quantifying the immobilized nanoparticles by digesting each well with acids and analyzing the gold content through inductively coupled plasma mass spectrometry (ICP-MS). We found that Fibronectin, Factor V, Antithrombin III, Complement C3, complement factor H, and IgG comprised 87% of all the tested functional proteins (Figure S11). When we combined the functional concentration of 24 proteins and compared it to the total amount of adsorbed 24 tested proteins, we found that it only adds up to 27.4% (Figure 2C). This suggests that a large portion of proteins are not functional for binding. Though other factors such as orientation and unfolding of the protein may contribute to this low binding function,[27,28] we suspect that the organization of proteins in the protein corona structure is preventing them from being accessible for binding.

The fact that many of the proteins are not available for binding suggests that the proteins may have been organized into multiple layers. The current view of the protein corona's structure is a monolayer of adsorbed proteins, but few studies have suggested that the protein corona is a multilayered system.[29−33] A multilayer structure hints at strong protein−protein interactions. We designed an assay that allows us to screen for such interactions by isolating proteins in their native structure. Current methods of isolating proteins often require denaturation that disrupts their structural conformation. We chose the iodine and iodide ion-based chemical etchant to dissolve the gold nanoparticles to release adsorbed proteins without affecting the native structure of proteins.[34,46] The experimental overview of our method is shown schematically in Figure 3A. We first tested and validated the etching process using a model IgG-coated gold nanoparticles (IgG-NPs) construct.

60 nm gold nanoparticles were synthesized and incubated with IgG. Once the IgG was adsorbed on the surface, we removed the excessive unbound IgG by centrifuging and washed the IgG-NPs with PBST. The etchant was then prepared by mixing the iodine with 530 mM of potassium iodide solution at 10% v/v. We added the etchant to the IgG-NPs solution and immediately started following its adsorption spectrum. As shown in Figure 3B, the absorption peak of nanoparticles around 535 nm quickly disappears once the etchant was added to the solution. There is only the peak of unreacted diiodine (I_2) at 250 nm after 10 min indicating the nanoparticles have been removed and the etching process is completed. We quenched the unreacted diiodine by adding sodium thiosulfate ($Na_2S_2O_3$). The adsorption peak of diiodine disappeared and left the solution colorless. We tested whether this etching process influences the function of proteins using ELISA. We compared the ELISA signal of etchant-treated IgG with the untreated ones and found that they are similar (Figure 3C). This indicates that the etchant does not interfere with the ELISA assay, and the proteins can bind to their target after the treatment. We next validated that the number of released IgG matches with the initial adsorbed amount on the nanoparticle surface. We took the etched solution of IgG-NPs and quantified the number of IgG desorbed from the solution with ELISA. We also quantified the

https://dx.doi.org/10.1021/jacs.0c01853
J. Am. Chem. Soc. 2020, 142, 8827−8836

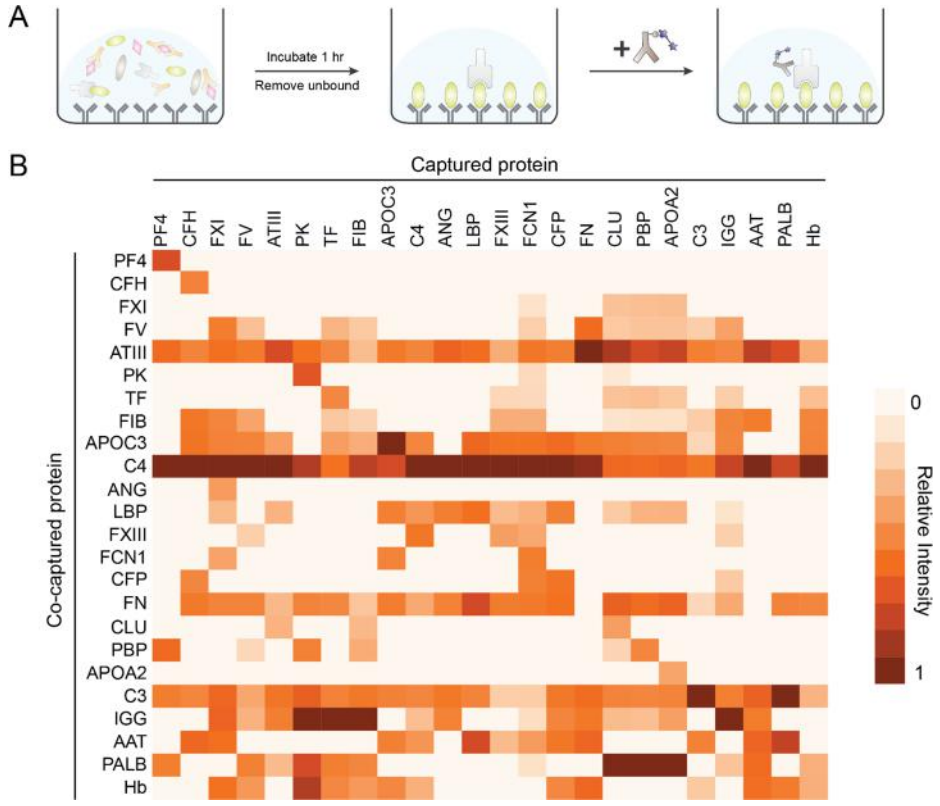

Figure 4. Identifying the structural organization of adsorbed proteins in the protein corona. (A) Schematics of the screening assay for identifying the protein binding pairs. Proteins in their native structure were desorbed from the nanoparticle surface through chemically etching away the gold core. The target protein was immobilized onto the wells by its antibody. Co-immobilized proteins were identified through screening with 24 different proteins' biotinylated antibody. Avidin-conjugated HRP was added, and a colorimetric signal at 450 nm was measured after adding the substrate 3,3′,5,5′-Tetramethylbenzidine (TMB). (B) The binding map of the 24 adsorbed proteins. Each column represents the immobilized protein, and each row represents the proteins that were coimmobilized. The colorimetric signal was normalized to the maximum within each target protein.

amount that is initially adsorbed on nanoparticles by the traditional method of desorbing IgG through denaturation with sodium dodecyl sulfate and dithiothreitol. The released IgG using this method was quantified with bicinchoninic acid assay as described in the previous study by Walkey et al.[19] We compared the two results and found that they are similar (Figure 3D). This indicates that we can release all adsorbed proteins with the iodine etchant. At last, we showed that the protein−protein binding remains intact after the etching. We prepared IgG-NPs that are bound with anti-IgG-HRP (Figure S12). We then etched the gold core and added the released protein mixture to an anti-IgG precoated well. The well will only immobilize the IgG. We found that the anti-IgG-HRP are coimmobilized onto the well after the etching (Figure S12c). This demonstrates that the IgG and anti-IgG-HRP remained bound after the etching process. After these validations, we applied the etchant to serum protein-coated nanoparticles and identified the protein−protein pairs in the released proteins.

Protein−protein binding pairs were identified using the immunoassay as schematically shown in Figure 4A. We first prepared the human serum protein-coated nanoparticles (HS-NPs) by incubating 60 nm gold nanoparticles with the serum. We added the etchant described above to HS-NPs to release all the adsorbed proteins. We tested whether there is any protein−protein binding in the released proteins. The protein solution was added to the well plates that were precoated with the antibody targeting one of the proteins in the list of 24 proteins. Such a procedure immobilized the target protein from the released protein mixture. This is a crucial step for identifying the protein−protein binding partners because if the target protein is bound with other proteins, the whole protein complex will be immobilized as well. We can then screen for which proteins have been coimmobilized by adding biotinylated antibodies for the protein partner. The antibody binds to one of the 24 proteins and can be recognized by adding avidin-HRP. The HRP generates a colorimetric readout with the absorbance at 450 nm allowing us to identify the coimmobilized proteins. For each protein in the list, we tested whether it is bound with all 24 proteins. Even though only the proteins within the list were tested, it still allows us to demonstrate the protein−protein interactions underlying the structural organization of the protein corona.

In total, we tested 24 × 24 = 576 pairs of proteins and identified which pair of proteins are bound together in the corona. We discovered 244 protein−protein binding pairs. This shows that 42% of the tested proteins are bound with other corona proteins. Antithrombin III, Apolipoprotein C3, Complement C4, Fibronectin, Complement C3, and IgG appeared in almost all protein−protein binding pairs. A binding map between the 24 proteins was constructed as shown in Figure 4B. Each column represents the protein that was immobilized on the plate, and each row represents the protein that was found coimmobilized. The intensity of each cell in the map shows the amount of each coimmobilized

https://dx.doi.org/10.1021/jacs.0c01853
J. Am. Chem. Soc. 2020, 142, 8827−8836

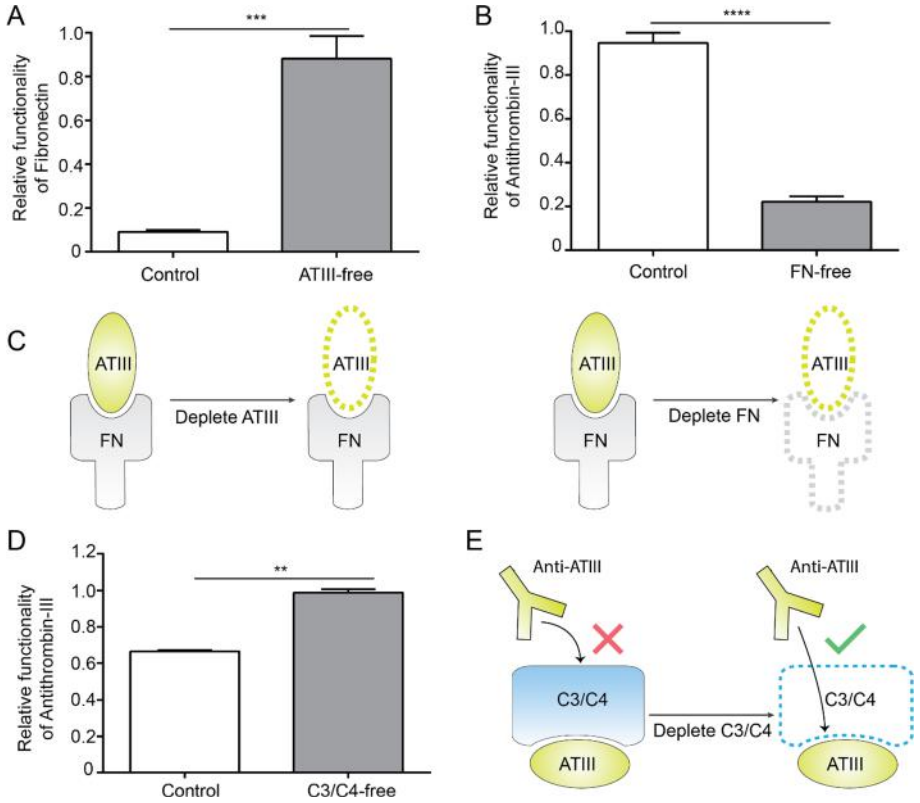

Figure 5. Manipulating the binding function of proteins through changing its structural organization in the protein corona. (A) The relative change in the amount of binding functional fibronectin (FN) on nanoparticles after antithrombin-III (ATIII) was depleted from the corona. This is compared to the control corona prepared from full human serum. (B) The relative change in the amount of binding functional ATIII on nanoparticles after FN was depleted from the corona. This is compared to the control corona prepared from full human serum. For both A and B, protein's relative binding functionality was determined through comparing the absorbance signal at 450 nm using the same ELISA method described earlier. (C) The proposed structural organization between ATIII and FN. ATIII binds to FN blocking its binding sites. FN, in turn, acts as the support for binding ATIII. (D) The relative change in the amount of binding functional ATIII on nanoparticles after complement protein C3 and C4 were depleted from the corona. This is also compared to the control corona prepared from full human serum. (E) The proposed structural organization between C3/C4 and ATIII. Complement protein C3 and C4 bind to ATIII blocking the binding sites of ATIII.

protein relative to other proteins in the same column. The binding pattern between proteins appeared to be nonsymmetrical. This suggests that the protein−protein interactions in the protein corona are not binary. This means multiple proteins can bind together to form an assembly. Multiple layers of proteins could be arranged under such a structure. Our findings also explain the fact that proteins lose their binding function as they are already bound to other corona proteins.

We tested whether we can manipulate the protein assemblies to control the binding function of a particular protein. We hypothesized that by removing one protein from a binding pair, it will influence the binding function of its binding partner. We first referred to the binding map constructed earlier and selected Antithrombin III (ATIII) and Fibronectin (FN) as the pair of proteins to study. Both proteins bound strongly to each other and are also abundant in the corona (Figure S13). We obtained human plasma with ATIII or FN immunodepleted and incubated them with 60 nm gold nanoparticles. The protein corona formed from the depleted plasma showed no significant difference in the total amount of adsorbed proteins (Figure S14). We measured the number of binding functional FN after ATIII is depleted. We found that the number of functional FN significantly increased ($p < 0.0005$) after ATIII was removed from the corona (Figure 5A). We suspect that in a native, full serum-protein corona, ATIII is bound to the already adsorbed FN and thus blocking its binding sites. We measured the amount of ATIII that is functional for binding after FN was removed. We found that the number of functional ATIII decreased ($p < 0.0005$) when FN was removed (Figure 5B). It is likely that FN acts as a supporting layer for the binding of ATIII and thus ATIII blocks the binding sites on FN as illustrated in Figure 5C. This result suggests that different protein species such as ATIII and FN may have different roles in forming the protein corona structure.

To further confirm this phenomenon, we studied another binding pair of proteins in the protein corona. It was reported that Complement proteins C3 and fragments of Complement C4 can covalently and nonspecifically bind to proteins on nanoparticles.[35] Existing proteins in the corona can act as a supporting layer for further binding of C3 and C4 fragments.[36,37] We hypothesized that the depletion of these two complement proteins should, in turn, allow its previously blocked proteins to become available for binding again. Depleting the supporting layer proteins, on the other hand, will not affect C3 and C4 as their binding is nonspecific. We tested this hypothesis. C3 and C4-depleted human serum were first obtained and incubated with the nanoparticles to form the C3/C4-free corona. We then measured the protein binding functionality of C3 and C4's binding pairs: ATIII, FN, and Fibrinogen (FIB). We found that the binding function of ATIII, FN, FIB increased by 1.5, 5.0, and 1.9 folds, respectively

https://dx.doi.org/10.1021/jacs.0c01853
J. Am. Chem. Soc. 2020, 142, 8827−8836

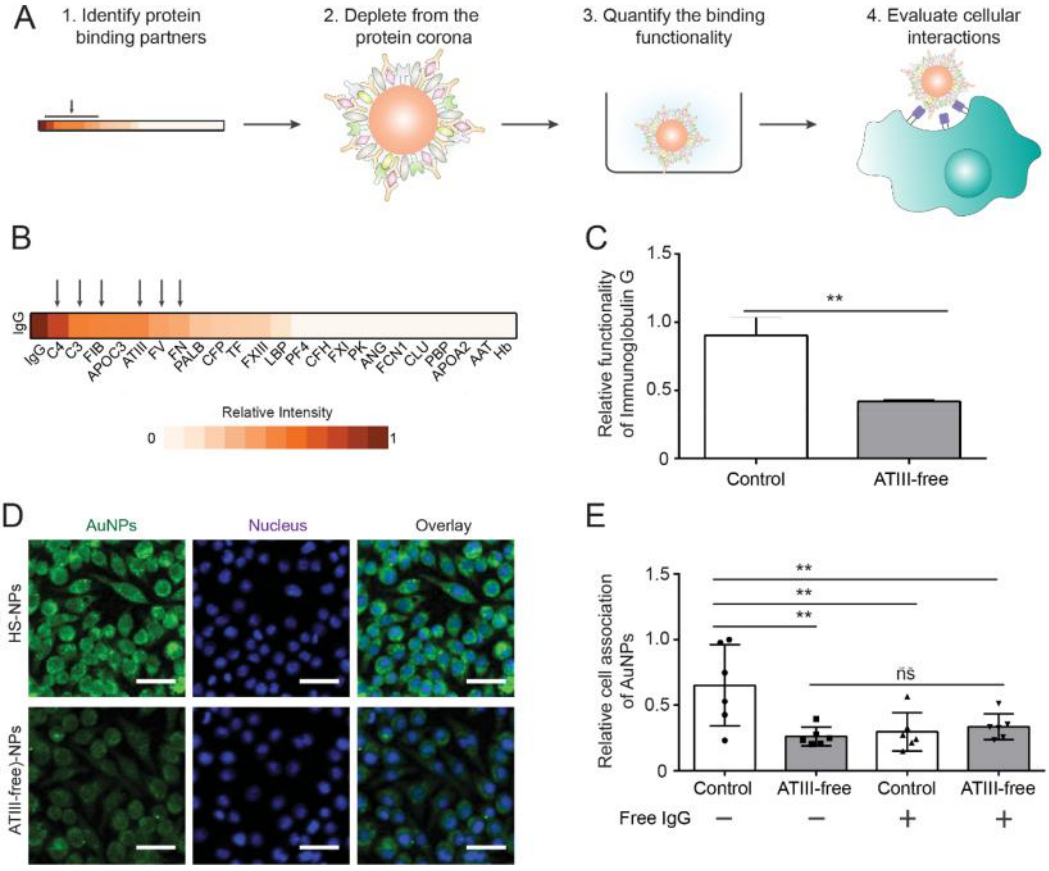

Figure 6. Modification of protein binding function on the protein corona termed Knockout Assisted Binding Activity Modification (KABAM). (A) Schematics of the KABAM. The binding partner of the protein of interest for modifying its binding function is first identified. The binding partners were depleted from the serum. The change in the binding functionality for the protein of interest is quantified through the ELISA assay described earlier. The changes in the cellular association of nanoparticles coated with the modified corona were evaluated. (B) Binding partners of the immunoglobulin G (IgG) in the protein corona of 60 nm gold nanoparticles. Serum or plasma with C3, C4, FIB, ATIII, FV, and FN depleted was purchased and incubated with nanoparticles to form the new corona. (C) The change in the number of binding functional IgG in the protein corona with ATIII depleted compared to the corona prepared from the full serum. (D) Confocal microscopy images of J774A.1 macrophage cells after incubation with human serum-coated nanoparticles (HS-NPs) and ATIII-free serum-coated nanoparticles (ATIII-free-NPs). The green channel shows staining for human IgG contained in the corona; the blue channel shows the nucleus of cells. Overlay images of both channels are presented in the right column. Scale bars are 40 μm. (E) Inductively coupled plasma mass spectrometry (ICP-MS) quantification of nanoparticles associated with cells. Nanoparticles with the full protein corona and corona with ATIII depleted were compared. The binding specificity to the receptor was confirmed through the binding completion with free IgG.

(Figure 5D, S15). However, we found that the amount of functional C3 and C4 did not change after ATIII, FN, and FIB were depleted from the corona (Figure S16). This agrees with the nonspecific binding nature of C3 and C4. Here we demonstrated that the binding properties of proteins can be controlled by manipulating the protein assemblies in the protein corona.

Finally, we evaluated whether we can manipulate the binding function of the corona to control nanoparticle-cell interactions. We picked nanoparticle-macrophage interaction as a model system. This is because macrophage cells are responsible for sequestering most nanomaterials.[38,39] The control of the interaction of nanoparticles with macrophage cells could lead to prolonged half-life in the body. Since FcγR is one of the major membrane receptors for binding to IgG,[40,41] we decided to alter the binding property of IgG in the nanoparticle's protein corona. We developed a workflow termed Knockout Assisted Binding Activity Modification (KABAM). As illustrated in Figure 6A, KABAM manipulates IgG's functionality by systematically depleting its binding pair and rearranging the corona. First, we selected candidate proteins from the binding map of IgG (Figure 6B). We found C3, C4, Antithrombin III, Fibronectin, Factor V, and Fibrinogen are the most significant proteins that bind IgG. We purchased depleted plasma for each one of these proteins. We incubated the 60 nm nanoparticles with the depleted plasma to form the new protein corona. To characterize the altered IgG functionality, we quantified the number of functional IgG in each protein corona using the ELISA assay. Figure 6C and Figure S17 show the amount of IgG that can bind to their target decreased after depleting Factor V, Fibrinogen, Antithrombin III, and Fibronectin. These proteins likely serve as the supporting proteins for IgG to bind to during the formation of the protein corona. On the other hand, the depletion of C3 and C4 leads to an increased number of IgG that can bind to their target (Figure S18). This agrees with our previous finding that C3 and C4 nonspecifically block the binding function of other proteins. Here, we engineered two new biological identities of protein corona that have enhanced or diminished IgG binding functionality using KABAM.

Next, we evaluated how these two protein corona control nanoparticles binding with macrophage cells. Nanoparticles

https://dx.doi.org/10.1021/jacs.0c01853
J. Am. Chem. Soc. 2020, 142, 8827–8836

with ATIII depleted corona have lower IgG binding ability and thus should have less binding with the cells, while C3/C4 depleted corona will have more. We first prepared J774.2 macrophage cells in serum-protein free media. Protein corona-coated nanoparticles were added to cells and allowed interaction for 30 min at 4 °C. We used a low temperature and short incubation time to minimize the contribution of receptor recycling.[47] Full human serum-coated nanoparticles were also incubated with cells under the same conditions to serve as the control. Microscopy images were taken to visualize the cellular binding of nanoparticles by labeling the protein corona with the anti-IgG conjugated with Cy5. Figure 6D shows nanoparticles with ATIII-free corona had much less fluorescence signal on macrophages than nanoparticles with the full corona. Using ICP-MS, we confirmed that the lack of signal is due to significantly less ($p < 0.005$) binding of nanoparticles to the cells (Figure 6E). We also added free human IgG to cells 10 min prior to the addition of nanoparticles. This allows us to confirm that the binding mechanism is through the Fc receptors. With the competition, serum corona-coated nanoparticles bind significantly less to macrophages, while no difference was observed for ATIII-free corona coated nanoparticles. We next tested the macrophage binding of nanoparticles with the C3/C4-free corona. We found that these nanoparticles with more binding functional IgG also bind significantly more ($p < 0.0005$) to macrophages (Figure S19). Here, we demonstrated that by modifying the organization of proteins in the corona, we can change the binding functionality of proteins. This leads to altered nanoparticles' cellular interactions. This new strategy allows us to control the biological identity of the protein corona without changing the physicochemical properties of the nanomaterials.

CONCLUSION

We characterized the binding functionality of proteins and started to examine their organization in the corona. We discovered that not all proteins in the protein corona can bind to their targets. Moreover, we found that proteins are organized into the assembly like structure through protein−protein interactions. This finding suggests a multilayered protein corona structure, as illustrated in Figure 7. Protein corona is likely composed of multilayers of protein assemblies. The foundational layer is defined as the layer of proteins that directly interact with the nanoparticle surface. The nanoparticle chemical composition and surface chemistries likely dictate the specific serum proteins adsorbed. This composition of this protein dictates the subsequent proteins adsorption on the nanoparticle surface, as these proteins can bind to cognate proteins. The cognate protein can potentially bind to additional proteins. We define these layers as the foundational, assembly, or binding layer when there are three proteins in the assembly. However, with two proteins interacting, there would only be a foundation and binding layer. In a one-protein layer, the binding layer is the same as the foundation layer. The assembly layer can constitute more than one protein. The outermost proteins are responsible for binding to cellular receptors. Finally, we demonstrated that we can manipulate the biological effect of a protein corona by changing the organization of proteins within it. We used this finding to develop a strategy termed Knockouts Assisted Binding Activity Modification (KABAM) to control the downstream biological interactions of nanoparticles with macrophages. This strategy allows us to control the biological identity of the protein corona without modifying the synthetic properties of the nanoparticle itself. This offers the tunability to the protein corona that could be used to engineer precoated corona with a variety of biological identities for nanomaterials.[42−45] Overall, this study provided insights into the structure and functionality of the protein corona that can be leveraged for the development of nanomaterials with controlled biological interactions.

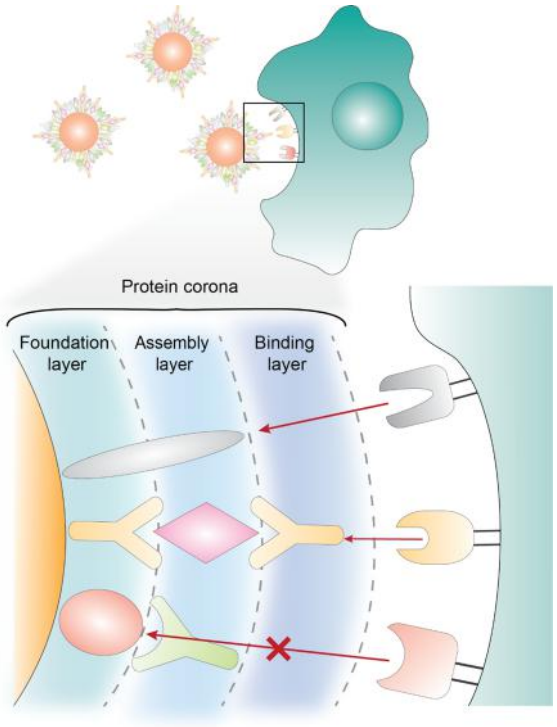

Figure 7. Proposed mechanism of the structure and function of the protein corona. This is an example of a three-layer, protein−protein−protein interaction. When nanoparticles are exposed to serum or plasma, proteins adsorb onto the surface through protein−nanoparticle interaction. It forms the foundation layer. Additional proteins can bind to the foundation layer of proteins based on protein−protein interactions. This forms the assembly layer. The protein that was sterically covered by other proteins loses their binding functionality to receptors as they are not accessible. As a result, the interaction between the nanoparticle protein corona and cellular receptors is ultimately determined by the functional proteins in the binding layer. There is only a foundation and binding layer when there is a two-layer protein−protein interaction. The foundation equals the binding layer when there is one protein. An assembly layer can constitute more than one protein (for example, a protein−protein−protein−protein system would have two proteins in the assembly layer).

ASSOCIATED CONTENT

Supporting Information

The Supporting Information is available free of charge at https://pubs.acs.org/doi/10.1021/jacs.0c01853.

Materials and methods, protein-coated nanoparticle characterization, the protein composition of the corona, immunoassay characterization, immunoassay validation with IgG-NP, etching validation, quantification of nanoparticles binding to cells, and other data as mentioned in the text (PDF)

https://dx.doi.org/10.1021/jacs.0c01853
J. Am. Chem. Soc. 2020, 142, 8827−8836

AUTHOR INFORMATION

Corresponding Author

Warren C. W. Chan − *Department of Chemistry, Institute of Biomaterials and Biomedical Engineering, Terrence Donnelly Centre for Cellular and Biomolecular Research, Department of Chemical Engineering, and Department of Materials Science and Engineering, University of Toronto, Toronto, Ontario M5S 3H6, Canada;* orcid.org/0000-0001-5435-4785; Email: warren.chan@utoronto.ca

Authors

Yuwei Zhang − *Department of Chemistry and Institute of Biomaterials and Biomedical Engineering, University of Toronto, Toronto, Ontario M5S 3H6, Canada*

Jamie L. Y. Wu − *Institute of Biomaterials and Biomedical Engineering and Terrence Donnelly Centre for Cellular and Biomolecular Research, University of Toronto, Toronto, Ontario M5S 3G9, Canada*

James Lazarovits − *Institute of Biomaterials and Biomedical Engineering and Terrence Donnelly Centre for Cellular and Biomolecular Research, University of Toronto, Toronto, Ontario M5S 3G9, Canada*

Complete contact information is available at: https://pubs.acs.org/10.1021/jacs.0c01853

Notes

The authors declare no competing financial interest.

ACKNOWLEDGMENTS

We thank the SPARC BioCentre at SickKids Hospital (Toronto) for the proteome analysis, Yih Yang Chen for the confocal microscopy images, and Ben Stordy for the TEM images, and Dr. Shrey Sindhwani reading and providing feedback on our manuscript. W.C.W.C. acknowledges the Canadian Institutes of Health Research (PJT-148848 and FDN-159932), Natural Sciences and Engineering Research Council of Canada (2015-0637); Canadian Research Chairs Program (950-223924); Nanomedicines Innovation Network NCE. Y.Z. thanks the Ontario Ministry of Training, Colleges and Universities and the University of Toronto for the Queen Elizabeth II Graduate Scholarship in Science and Technology. J.L.Y.W. thanks the Barbara & Frank Milligan Graduate Fellowship, Cecil Yip Doctoral Research Award, and the Canada Graduate Scholarship (NSERC).

REFERENCES

(1) Pelaz, B.; Alexiou, C.; Alvarez-Puebla, R. A.; Alves, F.; Andrews, A. M.; Ashraf, S.; Balogh, L. P.; Ballerini, L.; Bestetti, A.; Brendel, C.; Bosi, S.; Carril, M.; Chan, W. C. W.; Chen, C.; Chen, X.; Chen, X.; Cheng, Z.; Cui, D.; Du, J.; Dullin, C.; Escudero, A.; Feliu, N.; Gao, M.; George, M.; Gogotsi, Y.; Grünweller, A.; Gu, Z.; Halas, N. J.; Hampp, N.; Hartmann, R. K.; Hersam, M. C.; Hunziker, P.; Jian, J.; Jiang, X.; Jungebluth, P.; Kadhiresan, P.; Kataoka, K.; Khademhosseini, A.; Kopeček, J.; Kotov, N. A.; Krug, H. F.; Lee, D. S.; Lehr, C.; Leong, K. W.; Liang, X.; Ling, L. M.; Liz-Marzán, L. M.; Ma, X.; Macchiarini, P.; Meng, H.; Möhwald, H.; Mulvaney, P.; Nel, A. E.; Nie, S.; Nordlander, P.; Okano, T.; Oliveira, J.; Park, T.; Penner, R. M.; Prato, M.; Puntes, V.; Rotello, V. M.; Samarakoon, A.; Schaak, R. E.; Shen, Y.; Sjöqvist, S.; Skirtach, A. G.; Soliman, M. G.; Stevens, M. M.; Sung, H.; Tang, B. Z.; Tietze, R.; Udugama, B. N.; VanEpps, J. S.; Weil, T.; Weiss, P. S.; Willner, I.; Wu, Y.; Yang, L.; Yue, Z.; Zhang, Q.; Zhang, Q.; Zhang, X.; Zhao, Y.; Zhou, X.; Parak, W. J. Diverse Applications of Nanomedicine. *ACS Nano* **2017**, *11*, 2313−2381.

(2) Kim, B. Y. S.; Rutka, J. T.; Chan, W. C. W. Nanomedicine. *N. Engl. J. Med.* **2010**, *363*, 2434−2443.

(3) Davis, M. E.; Chen, Z. G.; Shin, D. M. Nanoparticle Therapeutics: An Emerging Treatment Modality for Cancer. *Nat. Rev. Drug Discovery* **2008**, *7*, 771−782.

(4) Perrault, S. D.; Walkey, C.; Jennings, T.; Fischer, H. C.; Chan, W. C. W. Mediating Tumor Targeting Efficiency of Nanoparticles through Design. *Nano Lett.* **2009**, *9*, 1909−1915.

(5) Choi, C. H. J.; Alabi, C. A.; Webster, P.; Davis, M. E. Mechanism of Active Targeting in Solid Tumors with Transferrin-Containing Gold Nanoparticles. *Proc. Natl. Acad. Sci. U. S. A.* **2010**, *107*, 1235−1240.

(6) Feng, Q.; Liu, Y.; Huang, J.; Chen, K.; Huang, J.; Xiao, K. Uptake, Distribution, Clearance, and Toxicity of Iron Oxide Nanoparticles with Different Sizes and Coatings. *Sci. Rep.* **2018**, *8*, 2082.

(7) Chen, L.; Zhou, S.; Su, L.; Song, J. Gas-Mediated Cancer Bioimaging and Therapy. *ACS Nano* **2019**, *13*, 10887−10917.

(8) Wong, X. Y.; Sena-Torralba, A.; Alvarez-Diduk, R.; Muthoosamy, K.; Merkoci, A. *ACS Nano* **2020**, *14*, 2585−2627.

(9) Cedervall, T.; Lynch, I.; Lindman, S.; Berggård, T.; Thulin, E.; Nilsson, H.; Dawson, K. A.; Linse, S. Understanding the Nanoparticle-Protein Corona Using Methods to Quantify Exchange Rates and Affinities of Proteins for Nanoparticles. *Proc. Natl. Acad. Sci. U. S. A.* **2007**, *104*, 2050−2055.

(10) del Pino, P.; Pelaz, B.; Zhang, Q.; Maffre, P.; Nienhaus, G. U.; Parak, W. J. Protein Corona Formation around Nanoparticles − from the Past to the Future. *Mater. Horiz.* **2014**, *1*, 301−313.

(11) Ke, P. C.; Lin, S.; Parak, W. J.; Davis, T. P.; Caruso, F. A Decade of the Protein Corona. *ACS Nano* **2017**, *11*, 11773−11776.

(12) Docter, D.; Westmeier, D.; Markiewicz, M.; Stolte, S.; Knauer, S. K.; Stauber, R. H. The Nanoparticle Biomolecule Corona: Lessons Learned − Challenge Accepted? *Chem. Soc. Rev.* **2015**, *44*, 6094−6121.

(13) Salvati, A.; Pitek, A. S.; Monopoli, M. P.; Prapainop, K.; Bombelli, F. B.; Hristov, D. R.; Kelly, P. M.; Åberg, C.; Mahon, E.; Dawson, K. A. Transferrin-Functionalized Nanoparticles Lose Their Targeting Capabilities When a Biomolecule Corona Adsorbs on the Surface. *Nat. Nanotechnol.* **2013**, *8*, 137−143.

(14) Walczyk, D.; Bombelli, F. B.; Monopoli, M. P.; Lynch, I.; Dawson, K. A. What the Cell "Sees" in Bionanoscience. *J. Am. Chem. Soc.* **2010**, *132*, 5761−5768.

(15) Lundqvist, M.; Stigler, J.; Elia, G.; Lynch, I.; Cedervall, T.; Dawson, K. A. Nanoparticle Size and Surface Properties Determine the Protein Corona with Possible Implications for Biological Impacts. *Proc. Natl. Acad. Sci. U. S. A.* **2008**, *105*, 14265−14270.

(16) Lazarovits, J.; Sindhwani, S.; Tavares, A. J.; Zhang, Y.; Song, F.; Audet, J.; Krieger, J. R.; Syed, A. M.; Stordy, B.; Chan, W. C. W. Supervised Learning and Mass Spectrometry Predicts the in Vivo Fate of Nanomaterials. *ACS Nano* **2019**, *13*, 8023−8034.

(17) Chonn, A.; Semple, S. C.; Cullis, P. R. Association of Blood Proteins with Large Unilamellar Liposomes in Vivo. Relation to Circulation Lifetimes. *J. Biol. Chem.* **1992**, *267*, 18759−18765.

(18) Tenzer, S.; Docter, D.; Kuharev, J.; Musyanovych, A.; Fetz, V.; Hecht, R.; Schlenk, F.; Fischer, D.; Kiouptsi, K.; Reinhardt, C.; Landfester, K.; Schild, H.; Maskos, M.; Knauer, S. K.; Stauber, R. H. Rapid Formation of Plasma Protein Corona Critically Affects Nanoparticle Pathophysiology. *Nat. Nanotechnol.* **2013**, *8*, 772−781.

(19) Walkey, C. D.; Olsen, J. B.; Guo, H.; Emili, A.; Chan, W. C. W. Nanoparticle Size and Surface Chemistry Determine Serum Protein Adsorption and Macrophage Uptake. *J. Am. Chem. Soc.* **2012**, *134*, 2139−2147.

(20) Walkey, C. D.; Olsen, J. B.; Song, F.; Liu, R.; Guo, H.; Olsen, D. W. H.; Cohen, Y.; Emili, A.; Chan, W. C. W. Protein Corona Fingerprinting Predicts the Cellular Interaction of Gold and Silver Nanoparticles. *ACS Nano* **2014**, *8*, 2439−2455.

(21) Bertrand, N.; Grenier, P.; Mahmoudi, M.; Lima, E. M.; Appel, E. A.; Dormont, F.; Lim, J.-M.; Karnik, R.; Langer, R.; Farokhzad, O. C. Mechanistic Understanding of in Vivo Protein Corona Formation

on Polymeric Nanoparticles and Impact on Pharmacokinetics. *Nat. Commun.* **2017**, *8*, 777.
(22) García-Álvarez, R.; Hadjidemetriou, M.; Sánchez-Iglesias, A.; Liz-Marzán, L. M.; Kostarelos, K. In Vivo Formation of Protein Corona on Gold Nanoparticles. The Effect of Their Size and Shape. *Nanoscale* **2018**, *10*, 1256−1264.
(23) Kelly, P. M.; Åberg, C.; Polo, E.; O'Connell, A.; Cookman, J.; Fallon, J.; Krpetić, Ž.; Dawson, K. A. Mapping Protein Binding Sites on the Biomolecular Corona of Nanoparticles. *Nat. Nanotechnol.* **2015**, *10*, 472−479.
(24) Clemments, A. M.; Botella, P.; Landry, C. C. Spatial Mapping of Protein Adsorption on Mesoporous Silica Nanoparticles by Stochastic Optical Reconstruction Microscopy. *J. Am. Chem. Soc.* **2017**, *139*, 3978−3981.
(25) Engvall, E.; Perlmann, P. Enzyme-Linked Immunosorbent Assay (ELISA) Quantitative Assay of Immunoglobulin G. *Mol. Immunol.* **1971**, *109*, 871−874.
(26) Bally, R. W.; Gribnau, T. C. J. Some Aspects of the Chromogen 3,3′,5,5′-Tetramethylbenzidine as Hydrogen Donor in a Horseradish Peroxidase Assay. *Clin. Chem. Lab. Med.* **1989**, *27*, 791−796.
(27) Deng, Z. J.; Liang, M.; Monteiro, M.; Toth, I.; Minchin, R. F. Nanoparticle-Induced Unfolding of Fibrinogen Promotes Mac-1 Receptor Activation and Inflammation. *Nat. Nanotechnol.* **2011**, *6*, 39−44.
(28) Cukalevski, R.; Lundqvist, M.; Oslakovic, C.; Dahlbäck, B.; Linse, S.; Cedervall, T. Structural Changes in Apolipoproteins Bound to Nanoparticles. *Langmuir* **2011**, *27*, 14360−14369.
(29) Simberg, D.; Park, J.-H.; Karmali, P. P.; Zhang, W.-M.; Merkulov, S.; McCrae, K.; Bhatia, S. N.; Sailor, M.; Ruoslahti, E. Differential Proteomics Analysis of the Surface Heterogeneity of Dextran Iron Oxide Nanoparticles and the Implications for Their in Vivo Clearance. *Biomaterials* **2009**, *30*, 3926−3933.
(30) Hellstrand, E.; Lynch, I.; Andersson, A.; Drakenberg, T.; Dahlbäck, B.; Dawson, K. A.; Linse, S.; Cedervall, T. Complete High-Density Lipoproteins in Nanoparticle Corona. *FEBS J.* **2009**, *276*, 3372−3381.
(31) Gagner, J. E.; Lopez, M. D.; Dordick, J. S.; Siegel, R. W. Effect of Gold Nanoparticle Morphology on Adsorbed Protein Structure and Function. *Biomaterials* **2011**, *32*, 7241−7252.
(32) Piella, J.; Bastús, N. G.; Puntes, V. Size-Dependent Protein-Nanoparticle Interactions in Citrate-Stabilized Gold Nanoparticles: The Emergence of the Protein Corona. *Bioconjugate Chem.* **2017**, *28*, 88−97.
(33) Goy-López, S.; Juárez, J.; Alatorre-Meda, M.; Casals, E.; Puntes, V. F.; Taboada, P.; Mosquera, V. Physicochemical Characteristics of Protein-NP Bioconjugates: The Role of Particle Curvature and Solution Conditions on Human Serum Albumin Conformation and Fibrillogenesis Inhibition. *Langmuir* **2012**, *28*, 9113−9126.
(34) Ramachandran, L. K. Protein-Iodine Interaction. *Chem. Rev.* **1956**, *56*, 199−218.
(35) Law, S. K.; Dodds, A. W. The Internal Thioester and the Covalent Binding Properties of the Complement Proteins C3 and C4. *Protein Sci.* **1997**, *6*, 263−274.
(36) Chen, F.; Wang, G.; Griffin, J. I.; Brenneman, B.; Banda, N. K.; Holers, V. M.; Backos, D. S.; Wu, L.; Moghimi, S. M.; Simberg, D. Complement Proteins Bind to Nanoparticle Protein Corona and Undergo Dynamic Exchange in Vivo. *Nat. Nanotechnol.* **2017**, *12*, 387−393.
(37) Vu, V. P.; Gifford, G. B.; Chen, F.; Benasutti, H.; Wang, G.; Groman, E. V.; Scheinman, R.; Saba, L.; Moghimi, S. M.; Simberg, D. Immunoglobulin Deposition on Biomolecule Corona Determines Complement Opsonization Efficiency of Preclinical and Clinical Nanoparticles. *Nat. Nanotechnol.* **2019**, *14*, 260−268.
(38) Yu, M.; Zheng, J. Clearance Pathways and Tumor Targeting of Imaging Nanoparticles. *ACS Nano* **2015**, *9*, 6655−6674.
(39) Wilhelm, S.; Tavares, A. J.; Dai, Q.; Ohta, S.; Audet, J.; Dvorak, H. F.; Chan, W. C. W. Analysis of Nanoparticle Delivery to Tumours. *Nat. Rev. Mater.* **2016**, *1*, 16014.
(40) Gallo, P.; Gonçalves, R.; Mosser, D. M. The Influence of IgG Density and Macrophage Fc (gamma) Receptor Cross-Linking on Phagocytosis and IL-10 Production. *Immunol. Lett.* **2010**, *133*, 70−77.
(41) Nimmerjahn, F.; Ravetch, J. V. Fc-Receptors as Regulators of Immunity. *Adv. Immunol.* **2007**, *96*, 179−204.
(42) Mirshafiee, V.; Kim, R.; Park, S.; Mahmoudi, M.; Kraft, M. L. Impact of Protein Pre-Coating on the Protein Corona Composition and Nanoparticle Cellular Uptake. *Biomaterials* **2016**, *75*, 295−304.
(43) Tonigold, M.; Simon, J.; Estupiñán, D.; Kokkinopoulou, M.; Reinholz, J.; Kintzel, U.; Kaltbeitzel, A.; Renz, P.; Domogalla, M. P.; Steinbrink, K.; Lieberwirth, I.; Crespy, D.; Landfester, K.; Mailänder, V. Pre-Adsorption of Antibodies Enables Targeting of Nanocarriers despite a Biomolecular Corona. *Nat. Nanotechnol.* **2018**, *13*, 862−869.
(44) Belling, J. N.; Jackman, J. A.; Yorulmaz Avsar, S.; Park, J. H.; Wang, Y.; Potroz, M. G.; Ferhan, A. R.; Weiss, P. S.; Cho, N.-J. Stealth Immune Properties of Graphene Oxide Enabled by Surface-Bound Complement Factor H. *ACS Nano* **2016**, *10*, 10161−10172.
(45) Prozeller, D.; Pereira, J.; Simon, J.; Mailänder, V.; Morsbach, S.; Landfester, K. Prevention of Dominant IgG Adsorption on Nanocarriers in IgG-Enriched Blood Plasma by Clusterin Precoating. *Adv. Sci.* **2019**, *6*, 1802199.
(46) Lazarovits, J.; Chen, Y. Y.; Song, J.; Ngo, W.; Tavares, A. J.; Zhang, Y. N.; Audet, J.; Tang, B.; Lin, Q.; Tleugabulova, M. C.; Wilhelm, S.; Krieger, J. R.; Mallevaey, T.; Chan, W. C. W. Synthesis of Patient-Specific Nanomaterials. *Nano Lett.* **2019**, *19*, 116−123.
(47) Mellman, I.; Plutner, H.; Ukkonen, P. Internalization and Rapid Recycling of Macrophage Fc Receptors Tagged with Monovalent Antireceptor Antibody: Possible Role of a Prelysosomal Compartment. *J. Cell Biol.* **1984**, *98*, 1163−1169.

https://dx.doi.org/10.1021/jacs.0c01853
J. Am. Chem. Soc. 2020, 142, 8827−8836